frontiers | Frontiers in Physics

TYPE Original Research
PUBLISHED 22 February 2023
DOI 10.3389/fphy.2023.1082086

Check for updates

OPEN ACCESS

EDITED BY
Bertrand Kibler,
UMR6303 Laboratoire Interdisciplinaire Carnot de Bourgogne (ICB), France

REVIEWED BY
Jingjing Zheng,
Beijing Jiaotong University, China
Koustav Dey,
National Institute of Technology Warangal, India
Murugan Senthil Mani Rajan,
Anna University, India

*CORRESPONDENCE
Dong Zhi,
zhidong@cardc.cn

SPECIALTY SECTION
This article was submitted to Optics and Photonics, a section of the journal Frontiers in Physics

RECEIVED 27 October 2022
ACCEPTED 02 February 2023
PUBLISHED 22 February 2023

CITATION
Tao R, Huang L, Li M, Shen B, Feng X, Xie L, Weng J and Zhi D (2023), M^2 factor for evaluating fiber lasers from large mode area few-mode fibers.
Front. Phys. 11:1082086.
doi: 10.3389/fphy.2023.1082086

M^2 factor for evaluating fiber lasers from large mode area few-mode fibers

Rumao Tao[1], Long Huang[2], Min Li[1], Benjian Shen[1], Xi Feng[1], Lianghua Xie[1], Jin Weng[1] and Dong Zhi[2]*

[1]Laser Fusion Research Center, China Academy of Engineering Physics, Mianyang, China, [2]Hypervelocity Aerodynamics Institute, China Aerodynamics Research and Development Center, Mianyang, China

Evaluating the laser quality accurately is one of the most important and fundamental physical issues for laser sources, and the beam quality of lasers from the large mode area few-mode fibers have been haunted by the presence of high order mode for many years. This paper presents a modification to the M^2 factor, which can be used to evaluate the mode content of fiber lasers accurately and efficiently, no matter whether the fiber modes are superposited coherently or incoherently. By mathematical derivation, the origin of the influence of relative phase on the M^2 factor has been determined mathematically. A modification to the second moment of the beam intensity profile has been proposed, which eliminates the impact of uncontrollable relative phase on the second moment, and subsequently restores the one-to-one mapping between mode content and M^2 factor even for coherent superposition cases. Also presented are the results of numerical simulations, which support the validity of the modified M^2 factor to evaluate the mode content of the high power fiber lasers. With modified M^2 factor being less than 1.1, the power fraction of LP_{11} mode content is unique and determined to be less than 3%.

KEYWORDS

high power fiber lasers, large mode area fiber, few-mode fiber, beam quality, laser beam propagation

1 Introduction

Narrow Linewidth fiber laser systems, which have earned a solid reputation as a highly power scalable laser with excellent beam quality, are attractive sources for many applications, such as coherent lidar systems, nonlinear frequency conversion, and coherent/spectral beam combining architectures [1–4]. As the output power of fiber lasers grows into the multi-hundred range, detrimental nonlinear effects such as the stimulated Brillouin scattering (SBS) and the self-phase modulation (SPM) become the major limit factors that preclude further power upscaling [5]. Low numerical aperture (NA), large mode area (LMA) step index fiber designs, which support only a few modes in the core, have been employed to overcome the limitation of the nonlinear effects while maintaining a high beam quality of the output laser [6–10]. Various coiling of the fibers have been employed to filter the high order modes and achieve single mode (SM) operation in few-mode fiber [11–16], where criteria are required to evaluate the performance of these coiling tactic. After the introduce of M^2-factor, the M^2-factor has now become a indispensable standard of the laser beam quality in the fiber laser research and development, and the measured M^2-factor is nearly always specified to evaluate the fundamental mode (LP_{01}) purity whenever a new fiber laser source is demonstrated or produced. The M^2-factor is generally used to evaluate the fundamental mode purity in the aforementioned tactic of achieving SM operation in LMA fibers [11–16], and low M^2 values have been taken to imply that the near-SM or near-diffraction-limited performance is achieved: lower M^2 values means higher fraction of fundamental mode content in LMA fibers. Although the M^2 values of the fundamental mode is about 1, it does not means that the laser contains more fundamental mode power by $M^2 \rightarrow 1$. In LMA fiber, the high order mode, especially LP_{11} mode, is hard to be eliminated completely [18, 19]. Coiling-induced bend loss increases with the order of the fiber mode, and the bend loss of LP_{11} mode is the lowest among the high order mode. Meanwhile, the fiber perturbations result in that the high order modes are continually repopulated due to coupling between the fundamental mode and the high order modes [17], which is the strongest for the LP_{11} mode. In the presence of LP_{11} mode, even the excellent beam quality ($M^2 < 1.1$) in LMA fibers does not guarantee low power fraction of LP_{11} mode when the modes are superposited coherently, which are generally true for the narrow linewidth fiber lasers [18]. Due to the presence of the relative phase between the fiber modes, there is no one-to-one mapping between the mode content and the M^2-factor for the coherent superposition cases [18, 20]. For certain superposition state in LMA fibers, the M^2 value can be as good as 1.08 for a fiber laser consists of 30% LP_{11} and 70% LP_{01} [18], which results in that the widely employed criteria is unable to evaluate the fiber laser mode purity performance, and limits the applications of high power fiber lasers in the cases requiring strict mode purity. To determine the fundamental mode content, sophisticated methods should be employed, such as spatially and spectrally resolved imaging, cross-correlated imaging, modal decomposition [21–25]. However, the aforementioned methods require specially designed experimental setups and complicated algorithms, and are not compatible with the standard measuring instruments in laser industry [26, 27]. In recent years, some intelligent methods have been introduced to calculate the M^2-factor [28–30], which is still suffered from the problem induced by the presence of high order modes. A modification to the present method is simple and compatible with the standard measuring instruments, which inspires the work in this manuscript.

In this manuscript, the term that leads to the variation of the M^2 factor has been determined, and a modification to M^2 factor has been proposed to evaluate the beam quality or mode content of high power narrow linewidth laser from the LMA low NA step index fibers, which can mitigate the dependence of M^2 factor on the uncontrollable relative phase between the LP_{01} and LP_{11} modes, and restores the one-to-one mapping between the mode content and the M^2-factor for coherent superposition cases. Numerical simulations have been carried out to validate the modified M^2 factor, which revealed that the modified M^2 factor can be used to evaluate the mode content of fiber lasers, no matter whether the modes are superposited coherently or incoherently.

2 Theoretical model

As pointed out in [18, 19], for low NA, LMA fiber, LP_{11} mode is hard to be stripped totally and is the most problematic. In the following analysis, we focus our attention mainly on the case that only LP_{11} mode is contained in the laser, and the electric field of the high power fiber laser for narrow linewidth fiber laser can be expressed as [17]:

$$E(x,y,0) = \sqrt{1-P_{11}}\Psi_{LP_{01}}(x,y,0) + \sqrt{P_{11}}e^{i\Delta\phi_{11}}\Psi_{LP_{11}}(x,y,0), \quad (1)$$

where P_{11} is the power in the LP_{11} mode, and $\triangle\phi_{11}$ is the relative phase between the LP_{11} mode and the LP_{01} mode, which drift with fluctuations in temperature and other environmental factors, and are difficult to reliably control. In step index fibers, the normalized electric field of LP_{11} mode $\psi_{LPmn}(x, y, z = 0)$ can be written as:

$$\Psi_{LP_{mn}}(x,y,0) = \frac{f_{mn}(r)}{\sqrt{N_{mn}}}\cos(m\phi), \quad (2)$$

with

$$f_{mn}(r) = \frac{J_m(U_{mn}r/a)}{J_m(U_{mn})} \quad a \geq r > 0, \quad (3a)$$

$$f_{mn}(r) = \frac{K_m(W_{mn}r/a)}{K_m(W_{mn})} \quad r > a, \quad (3b)$$

where J_m and K_m is the Bessel function of the first kind and the modified Bessel function of the second kind, respectively, a is the core radius of the fiber, ($r = \sqrt{x^2+y^2}$, ϕ) is polar coordinates and λ is the wavelength. U_{mn} and W_{mn} are defined as in [31], and N_{mn} is the normalization factor, which can be expressed by:

$$N_{0n} = 2\pi\int_0^\infty f_{0n}^2(r)rdr \quad for\ m = 0, \quad (4a)$$

$$N_{mn} = \pi\int_0^\infty f_{mn}^2(r)rdr \quad for\ m > 0. \quad (4b)$$

According to Eq. 1, the intensity of the near field is given by:

$$\begin{aligned} I(x,y,0) = {} & P_{01}\Psi_{LP_{01}}^2(x,y,0) + P_{11}\Psi_{LP_{11}}^2(x,y,0) \\ & +2\sqrt{P_{01}P_{11}}\Psi_{LP_{01}}(x,y,0)\Psi_{LP_{11}} \\ & (x,y,0)\cos\Delta\phi_{11}, \end{aligned} \quad (5)$$

and the intensity of the field after propagating a distance of z is given by:

$$\begin{aligned} I(x,y,z) = {} & P_{01}\Psi_{LP_{01}}^2(x,y,z) + P_{11}\Psi_{LP_{11}}^2(x,y,z) \\ & +\sqrt{P_{01}P_{11}}\Psi_{LP_{01}}^*(x,y,z)\Psi_{LP_{11}}(x,y,z)e^{i\Delta\phi_{11}} \\ & +\sqrt{P_{01}P_{11}}\Psi_{LP_{01}}(x,y,z)\Psi_{LP_{11}}^*(x,y,z)e^{-i\Delta\phi_{11}}, \end{aligned} \quad (6)$$

where $\Psi_{LPmn}(x, y, z)$ is the field after $\Psi_{LPmn}(x, y, 0)$ propagates a distance of z. Then the M^2 factor is calculated by [32]:

$$M_x^2 = \left(\frac{\pi w_{0x}}{\lambda z}\right)\sqrt{w_{zx}^2 - w_{0x}^2}, \quad (7a)$$

$$M_y^2 = \left(\frac{\pi w_{0y}}{\lambda z}\right)\sqrt{w_{zy}^2 - w_{0y}^2}, \quad (7b)$$

with

$$w_{zx} = 2\sigma_{zx}, w_{zy} = 2\sigma_{zy}, \quad (8a)$$

$$\sigma_{zx}^2 = \frac{\int (x - x_0(z))^2 I(x,y,z)dxdy}{\int I(x,y,z)dxdy}, \quad (8b)$$

$$\sigma_{zy}^2 = \frac{\int (y - y_0(z))^2 I(x,y,z)dxdy}{\int I(x,y,z)dxdy}, \quad (8c)$$

$$w_{0x} = 2\sigma_{0x}, w_{0y} = 2\sigma_{0y}, \quad (8d)$$

$$\sigma_{0x}^2 = \frac{\int (x - x_0(0))^2 I(x,y,0)dxdy}{\int I(x,y,0)dxdy}, \quad (8e)$$

$$\sigma_{0y}^2 = \frac{\int (y - y_0(0))^2 I(x,y,0)dxdy}{\int I(x,y,0)dxdy}, \quad (8f)$$

where $\sigma_{zx(y)}$ and $w_{zx(y)}$ is the second moment of the beam intensity profile and the beam size at the distance of z along $x(y)$ direction, respectively, which is $\sigma_{0x(y)}$ and $w_{0x(y)}$ at the near filed. $(x_0(z), y_0(z))$ is the gravity center of the beam at the distance of z, given by:

$$x_0 = \frac{\int xIdxdy}{\int Idxdy}, \quad (9a)$$

$$y_0 = \frac{\int yIdxdy}{\int Idxdy}, \quad (9b)$$

where I is the laser intensity at arbitrary distance. In Eq. 7a, one can see that the M^2 seems to be dependent on the wavelength. However, the $w_{zx(y)}$ is also related to the wavelength through the laser intensity I. In fiber waveguide, the variation of the wavelength changes the V-number, which results in the laser intensity I changes. It is shown that the M^2 sharply peaks near the corresponding cutoff values of the V-number but remains nearly constant for V>3 [20]. In the practical high power laser systems, the V is generally larger than 3, so the dependence of M^2 on wavelength is negligible. The divergence angle of the beam can be obtained directly from M^2 value by employing the simple Equation in [33].

The second moment of the beam intensity profile can be expressed as:

$$\sigma_{zx}^2 = \frac{\int x^2 Idxdy}{\int Idxdy} + \frac{x_0^2 \int Idxdy}{\int Idxdy} - 2\frac{x_0 \int xIdxdy}{\int Idxdy}, \quad (10a)$$

$$\sigma_{zy}^2 = \frac{\int y^2 Idxdy}{\int Idxdy} + \frac{y_0^2 \int Idxdy}{\int Idxdy} - 2\frac{y_0 \int yIdxdy}{\int Idxdy}, \quad (10b)$$

According to the electric field distribution of the LP_{01} mode and the LP_{11} mode, we can obtain:

$$\Psi_{LP_{01}}(-x,y,0) = \Psi_{LP_{01}}(x,y,0), \quad (11)$$

and

$$\Psi_{LP_{11}}(x,y,0) = -\Psi_{LP_{11}}(-x,y,0), \quad (12)$$

where the LP_{11} mode is assumed to be anti-symmetric along x direction.

By using the extended Huygens–Fresnel principle [34–38], the electric field of the modes at the z plane can be expressed as:

$$\Psi_{LP_{01}}(p,q,z) = \frac{k}{2\pi z}\int_{-\infty}^{\infty}\int_{-\infty}^{\infty}\Psi_{LP_{01}}(x,y,0)\exp\left\{\frac{ik}{2z}\left[(p-x)^2+(q-y)^2\right]\right\}dxdy, \quad (13a)$$

$$\Psi_{LP_{11}}(p,q,z) = \frac{k}{2\pi z}\int_{-\infty}^{\infty}\int_{-\infty}^{\infty}\Psi_{LP_{11}}(x,y,0)\exp\left\{\frac{ik}{2z}\left[(p-x)^2+(q-y)^2\right]\right\}dxdy, \quad (13b)$$

where (p, q) is the coordinate at the z plane. Then we can derive:

$$\Psi_{LP_{01}}(-p,q,z) = \frac{k}{2\pi z}\int_{-\infty}^{\infty}\int_{-\infty}^{\infty}\Psi_{LP_{01}}(x,y,0)\exp\left\{\frac{ik}{2z}\left[(-p-x)^2+(q-y)^2\right]\right\}dxdy \overset{\xi=-x}{=} -\frac{k}{2\pi z}\int_{-\infty}^{\infty}\int_{-\infty}^{\infty}\Psi_{LP_{01}}(-\xi,y,0)\exp\left\{\frac{ik}{2z}\left[(-p+\xi)^2+(q-y)^2\right]\right\}d\xi dy, \quad (14a)$$

$$\Psi_{LP_{11}}(-p,q,z) = \frac{k}{2\pi z}\int_{-\infty}^{\infty}\int_{-\infty}^{\infty}\Psi_{LP_{11}}(x,y,0)\exp\left\{\frac{ik}{2z}\left[(-p-x)^2+(q-y)^2\right]\right\}dxdy \overset{\xi=-x}{=} -\frac{k}{2\pi z}\int_{-\infty}^{\infty}\int_{-\infty}^{\infty}\Psi_{LP_{11}}(-\xi,y,0)\exp\left\{\frac{ik}{2z}\left[(-p+\xi)^2+(q-y)^2\right]\right\}d\xi dy, \quad (14b)$$

Take Eqs 11, 12 into consideration, the above equations can be rewritten as:

$$\Psi_{LP_{01}}(-p,q,z) = -\frac{k}{2\pi z}\int_{-\infty}^{\infty}\int_{-\infty}^{\infty}\Psi_{LP_{01}}(\xi,y,0)\exp\left\{\frac{ik}{2z}\left[(p-\xi)^2+(q-y)^2\right]\right\}d\xi dy, \quad (15a)$$

$$\Psi_{LP_{11}}(-p,q,z) = \frac{k}{2\pi z}\int_{-\infty}^{\infty}\int_{-\infty}^{\infty}\Psi_{LP_{11}}(\xi,y,0)\exp\left\{\frac{ik}{2z}\left[(p-\xi)^2+(q-y)^2\right]\right\}d\xi dy, \quad (15b)$$

which can be simplified into:

$$\Psi_{LP_{01}}(-p,q,z) = -\Psi_{LP_{01}}(p,q,z), \quad (16)$$

and

$$\Psi_{LP_{11}}(-p,q,z) = \Psi_{LP_{11}}(p,q,z), \quad (17)$$

Referring to the odd-even property, we can obtain:

$$\int\int \Psi_{LP_{01}}^*(x,y,z)\Psi_{LP_{11}}(x,y,z)dxdy = 0, \quad (18a)$$

$$\int\int \Psi_{LP_{01}}(x,y,z)\Psi_{LP_{11}}^*(x,y,z)dxdy = 0, \quad (18b)$$

$$\int\int x\Psi_{LP_{01}}^*(x,y,z)\Psi_{LP_{11}}(x,y,z)dxdy \neq 0, \quad (18c)$$

$$\int\int x\Psi_{LP_{01}}(x,y,z)\Psi_{LP_{11}}^*(x,y,z)dxdy \neq 0, \quad (18d)$$

$$\int\int x^2\Psi_{LP_{01}}^*(x,y,z)\Psi_{LP_{11}}(x,y,z)dxdy = 0, \quad (18e)$$

$$\int\int x^2\Psi_{LP_{01}}(x,y,z)\Psi_{LP_{11}}^*(x,y,z)dxdy = 0, \quad (18f)$$

According to Eq. 18a, one can conclude that only the third term in Eq. 10a is non-zero, which means that the third term introduces the effect of relative phase on the final obtained beam quality value. If we rewritten Eq. 10b as:

$$\sigma_{zx}^2 = \frac{\int x^2 Idxdy}{\int Idxdy}, \quad (19a)$$

$$\sigma_{zy}^2 = \frac{\int y^2 Idxdy}{\int Idxdy}, \quad (19b)$$

Eq. 7b becomes independent of the relative phase. Replacing the calculation equation of the second moment Eq. 10a with Eq. 19a, the

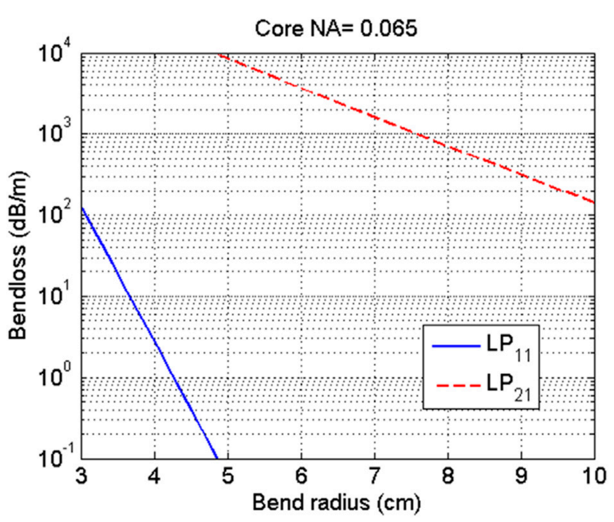

FIGURE 1
Bend loss vs. bend radius for different modes of a 0.065 NA fiber with a 30-μm-core at 1064 nm.

calculated M^2 factor is only dependent on the power content of LP_{11} mode, and the influence of relative phase on the M^2 factor is eliminated. By employing Eq. 19b, the influence of the last two terms in Eqs 5, 6, representing the mode interference, disappears, and the remaining terms is the same as the incoherent case. For the case that the modes are superposited incoherently, the gravity center of the beam is zero, Eq. 10b reduce to the form of Eq. 19a, and the modified M^2 factor in coherently superposited cases is coincident with those of the classical M^2 factor in incoherently superposited cases, which means that the ideal value for the modified M^2 factor is still very close to 1. In conclusion, the modified M^2 factor calculated from Eqs 7a, 19b can be used to evaluate the high power narrow linewidth fiber lasers.

3 Numerical simulations

For high power fiber lasers, nonlinear effects are the main limitation for power scaling, which is stronger for higher laser intensity [39]. Generally, fibers with larger core diameter have been employed to reduce the laser intensity in fiber core. However, the number of the supported modes in the core increases as the core diameter increases, which renders the fiber lasers into multimode operation, and undermines the beam quality [40]. To realize high power laser while maintaining near diffraction limited beam quality, a core diameter of 30 μm is generally used [41–47]. So the exemplary fiber that will be considered here has an ideal step-index profile with a 30 μm core and a core NA of 0.065, which was chosen to be representative of a commercially-

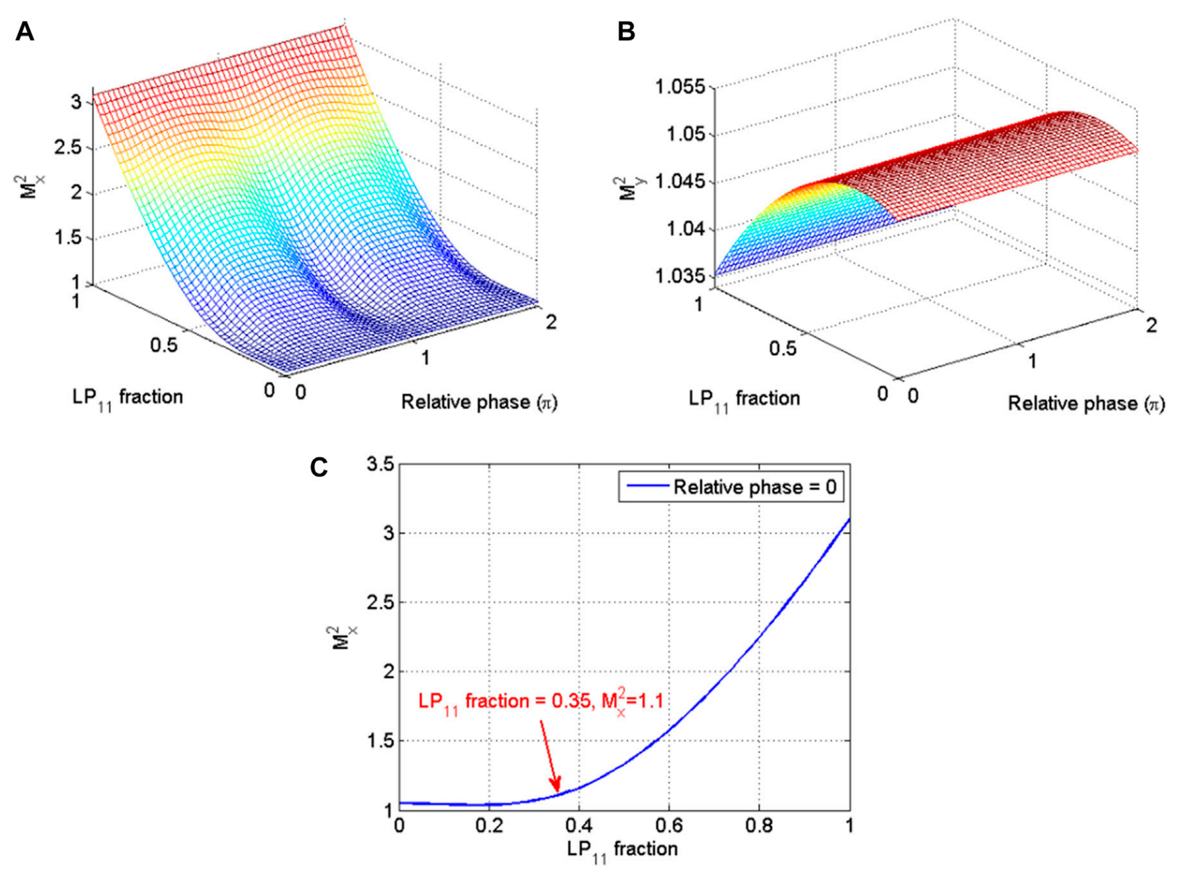

FIGURE 2
M^2 as a function of LP_{11} fraction and relative phase for x direction **(A)** and y direction **(B)**, M^2 as a function of LP_{11} fraction for the case that the relative phase is 0 **(C)**.

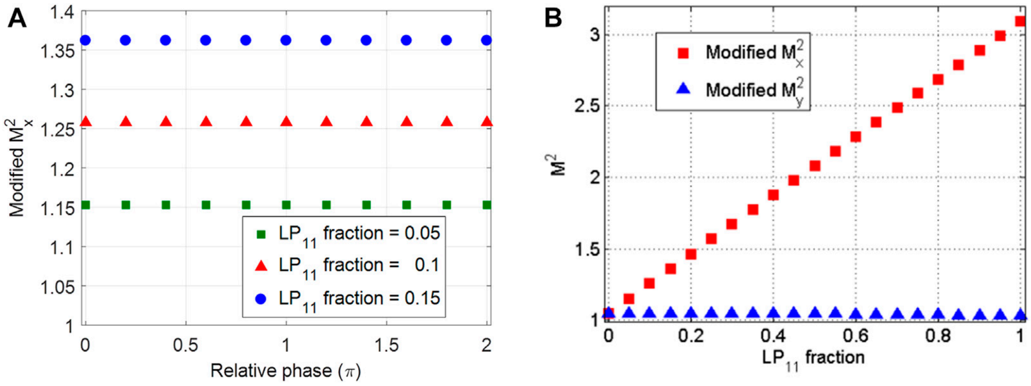

FIGURE 3
Beam quality factor of the coherent mixture of LP_{01} and LP_{11} modes, as a function of the relative phase **(A)** and higher order mode content **(B)**.

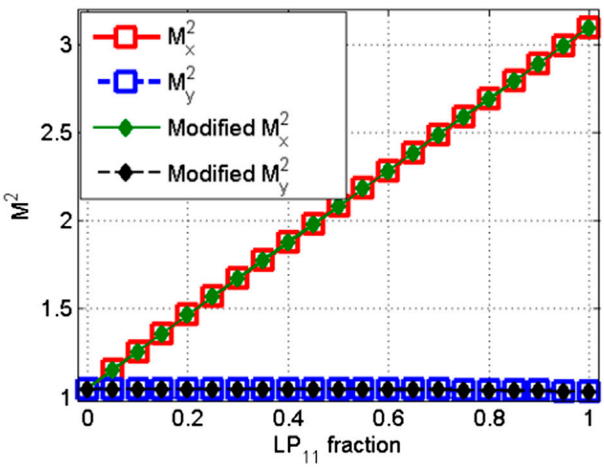

FIGURE 4
Beam quality factor of the incoherent mixture of LP_{01} and LP_{11} modes.

available LMA fiber and to validate the analysis in the former section. For high power narrow linewidth fiber lasers, the wavelength is generally located at 1064nm, and the laser wavelength used in simulation is chosen to be 1064 nm. The bend loss as a function of the bend radius for different modes is shown in Figure 1, which is calculated using the method of Marcuse [48]. An additional correction factor, yielding an effective bending diameter, has been employed to incorporate the material stress-optic effect [49]. It shows that even with the bend radius of 10cm, the bend loss for LP_{21} mode is significantly large, which is about 100 dB/m, which means that higher order mode can be stripped efficiently by coiling the fibers. For common fiber laser package of low NA LMA step index fiber, the bend radius of fiber is not larger than 10 cm to mitigating mode instability [6, 14], so it is reasonable to consider only the LP_{01} and LP_{11} mode.

We first calculated the M^2 factor by using the classical definition. The fiber mode profiles at the fiber output were propagated a distance from the initial plane ($z = 0$) by using the angular spectrum propagation method, which is based on fast Fourier Transform algorithm [50, 51]. Then several beam parameters of interest, such as second moment of the beam intensity profile and beam gravity centroid, can be calculated directly from the intensity distribution at the initial plane and distant plane, which are used to calculate the M^2 factor through Eqs 7a, 8a, 8b, 8c. The M^2 factor (in x and y direction) as a function of the LP_{11} fraction and the relative phase is calculated, which is shown in Figure 2. It is shown that the value of M^2 factor is dependent on the LP_{11} fraction and the relative phase, and M^2 is less than 1.1 even with the LP_{11} fraction as high as 0.35. It is indicated in [52] that the power in the bucket is dependent on the LP_{11} fraction, which means that even $M^2 < 1.1$ can not guarantee excellent long-distance propagation properties or high energy concentration for narrow width fiber laser, and that the M^2 factor can not reflect the mode content and is unsuitable to verify good propagation properties of a LMA fiber.

Employing the modified calculation, the modified M^2 factor as a function of relative phase and power fraction is presented in Figure 3. It can be seen from Figure 3A that the calculated M^2 factor is independent of the uncontrollable relative phase, which validate the predication in the theoretical analysis in Section 2. It also reveals in Figure 3B that the calculated modified M^2 factor increases linearly with the increase of high order mode content, which means that the M^2 factor can be used to evaluate the beam quality or mode content of the laser from low NA, LMA fibers. With modified M^2 factor being less than 1.1, the power fraction of LP_{11} mode content is less than 3%. In Figure 3B, the modified M_y^2 value is constant with a change in the LP_{11} fraction. This is due to that M^2 value in the y direction is nearly the same for LP_{01} mode and LP_{11} mode [20], and the modified M_y^2 value is a weighted superposition of the M^2 value for LP_{01} mode and LP_{11} mode.

The calculated M^2 factor as a function of power fraction is presented in Figure 4, in which the modes are superposited incoherently for the cases of broadband fiber lasers. Both classical and modified M^2 factor is used to evaluate the beam quality, which indicates that there is no difference in the two methods for the case that the modes are superposited incoherently. One can conclude that the modified M^2 factor is suitable for evaluating the beam quality of the fiber laser whenever the modes are superposited coherently or incoherently, which means that the methods can be employed in broader applications, not only restricted to evaluate the narrow linewidth fiber lasers but also the broadband ones. Due to that the modification is only made on the calculation of the second moment of the beam intensity profile, the modified M^2 can be used in the conventional measuring instrument except for updating the calculating software programs.

4 Conclusion

We have presented a modification to the M^2 factor for high power narrow linewidth lasers from low NA, LMA fibers. The modified M^2 factor eliminates the influence of the uncontrollable relative phase by ignoring the gravity center in the calculation of the beam intensity profile second moment, and the one-to-one mapping between the M^2 factor and the mode content has been restored, which make the M^2 factor can be employed to characterize the mode content even for the narrow linewidth fiber lasers. It is demonstrated numerically that the modification to M^2 factor can reflect the mode content, and the M^2 factor → 1 means that less high order mode are contained in the laser beam. With the new calculation method, the power fraction of LP_{11} mode is less than 3% when the modified M^2 parameter is less than 1.1. The results can be used to improve the method to measure the beam quality of high power fiber lasers.

Data availability statement

The raw data supporting the conclusion of this article will be made available by the authors, without undue reservation.

Author contributions

All authors listed have made a substantial, direct, and intellectual contribution to the study and approved it for publication.

Funding

This work was supported by the National Natural Science Foundation of China (NSFC) (61905226), and the Youth Talent Climbing Foundation of the Laser Fusion Research Center.

Conflict of interest

The authors declare that the research was conducted in the absence of any commercial or financial relationships that could be construed as a potential conflict of interest.

Publisher's note

References

1. Fu S, Shi W, Feng Y, Zhang L, Yang Z, Xu S, et al. Review of recent progress on single-frequency fiber lasers. *J Opt Soc Am B* (2017) 34(3):A49–A62. doi:10.1364/josab.34.000a49

2. Avdokhin A, Gapontsev V, Kadwani P, Vaupel A, Samartsev I, Platonov N, et al. High average power quasi-CW single-mode green and UV fiber lasers. *Proc SPIE* (2015) 9347:934704.

3. Honea E, Afzal RS, Savage-Leuchs M, Henrie J, Brar K, Kurz N, et al. Advances in fiber laser spectral beam combining for power scaling. *Proc SPIE* (2016) 9730:97300Y.

4. Flores A, Dajani I, Holten R, Ehrenreich T, Anderson B. Multi-kilowatt diffractive coherent combining of pseudorandom-modulated fiber amplifiers. *Opt Eng* (2016) 55: 096101. doi:10.1117/1.oe.55.9.096101

5. Dajani I, Flores A, Holten R, Anderson B, Pulford B, Ehrenreich T. Multi-kilowatt power scaling and coherent beam combining of narrow linewidth fiber lasers. *Proc SPIE* (2016) 9728:972801.

6. Tao R, Ma P, Wang X, Zhou P, Liu Z. 13 kW monolithic linearly polarized single-mode master oscillator power amplifier and strategies for mitigating mode instabilities. *Photon Res* (2015) 3:86–93. doi:10.1364/prj.3.000086

7. Ma P, Tao R, Su R, Wang X, Zhou P, Liu Z. 189 kW all-fiberized and polarization-maintained amplifiers with narrow linewidth and near-diffraction-limited beam quality. *Opt Express* (2016) 24:4187–95. doi:10.1364/oe.24.004187

8. Shen H, Lou Q, Quan Z, Li X, Yang Y, Chen X, et al. Narrow-linewidth all-fiber amplifier with up to 3.01 kW output power based on commercial 20/400 μm active fiber and counter-pumped configuration. *Appl Opt* (2019) 58:3053–8. doi:10.1364/ao.58.003053

9. Huang Z, Shu Q, Tao R, Chu Q, Luo Y, Yan D, et al. >5kW record high power narrow linewidth laser from traditional step-index monolithic fiber amplifier. *IEEE Photon Technol Lett* (2021) 33(21):1181–4. doi:10.1109/lpt.2021.3112270

10. Wang Y, Sun Y, Peng W, Feng Y, Wang J, Ma Y, et al. 3.25 kW all-fiberized and polarization-maintained Yb-doped amplifier with a 20 GHz linewidth and near-diffraction-limited beam quality. *Appl Opt* (2021) 60:6331–6. doi:10.1364/ao.431081

11. Limpert J, Liem A, Zellmer H, Tunnermann A. 500 W continuous wave fibre laser with excellent beam quality. *Electron Lett* (2003) 39:645–7. doi:10.1049/el:20030447

12. Koplow J, Kliner D, Goldberg L. Single-mode operation of a coiled multimode fiber amplifier. *Opt Lett* (2000) 25:442–4. doi:10.1364/ol.25.000442

13. Su R, Tao R, Wang X, Zhang H, Ma P, Zhou P, et al. 2.43 kW narrow linewidth linearly polarized all-fiber amplifier based on mode instability suppression. *Laser Phys Lett* (2017) 14:085102. doi:10.1088/1612-202x/aa760b085102

14. Tao R, Su R, Ma P, Wang X, Zhou P. Suppressing mode instabilities by optimizing the fiber coiling methods. *Laser Phys Lett* (2017) 14:025101. doi:10.1088/1612-202x/aa4fbf025101

15. Wang Y, Feng Y, Ma Y, Chang Z, Peng W, Sun Y, et al. 2.5 kW narrow linewidth linearly polarized all-fiber MOPA with cascaded phase-modulation to suppress SBS induced self-pulsing. *IEEE Photon J* (2020) 12:1–15. doi:10.1109/jphot.2020.2997935

16. Wang G, Song J, Chen Y, Ren S, Ma P, Liu W. 6 kW record all-fiberized and narrow-linewidth fiber amplifier with near-diffraction-limited beam quality. *High Power Laser Sci Eng* (2020) 1–14.

17. Rohrer C, Codemard CA, Kleem G, Graf T, Ahmed MA. Preserving nearly diffraction-limited beam quality over several hundred meters of transmission through highly multimode fibers. *J Lightwave Technol* (2019) 37:4260–7. doi:10.1109/jlt.2019.2922776

18. Wielandy S. Implications of higher-order mode content in large mode area fibers with good beam quality. *Opt Express* (2007) 15(23):15402–9. doi:10.1364/oe.15.015402

19. Huang L, Kong L, Leng J, Zhou P, Guo S, Cheng X. Impact of high-order-mode loss on high-power fiber amplifiers. *J Opt Soc Am B* (2016) 33:1030–7. doi:10.1364/josab.33.001030

20. Yoda H, Polynkin P, Mansuripur M. Beam quality factor of higher order modes in a step-index fiber. *J Lightwave Technol* (2006) 24(3):1350–5. doi:10.1109/jlt.2005.863337

21. Nicholson JW, Yablon AD, Ramachandran S, Ghalmi S. Spatially and spectrally resolved imaging of modal content in large-mode-area fibers. *Opt Express* (2008) 16: 7233–43. doi:10.1364/oe.16.007233

22. Schimpf DN, Barankov RA, Ramachandran S. Cross-correlated (C2) imaging of fiber and waveguide modes. *Opt Express* (2011) 19(14):13008–19. doi:10.1364/oe.19.013008

23. Stutzki F, Otto HJ, Jansen F, Gaida C, Jauregui C, Limpert J, et al. High-speed modal decomposition of mode instabilities in high-power fiber lasers. *Opt Lett* (2011) 36:4572–4. doi:10.1364/ol.36.004572

24. An Y, Huang L, Li J, Leng J, Yang L, Zhou P. Deep learning-based real-time mode decomposition for multimode fibers. *IEEE J Sel Top Quan Electron* (2020) 26:1–6. doi:10.1109/jstqe.2020.2969511

25. Zhang C, Chu Q, Feng X, Xie L, Liu Y, Li H. Mode evolution of high power monolithic PM fiber amplifiers in the presence of SRS effect. *IEEE Photon Technol Lett* (2022) 34:215–8. doi:10.1109/lpt.2022.3148999

26. Ophiropt. laser–measurement (2023). Available at: https://www.ophiropt.com/laser–measurement/beam-profilers/products/M2-Beam-Propagation-Analysis/BeamSquared (Accessed June 08, 2022).

27. Cinogy. cinsquare_m2_tool (2023). Available: http://www.cinogy.com/html/cinsquare_m2_tool.html (Accessed June 08, 2022).

28. An Y, Huang L, Li J, Leng J, Yang L, Zhou P. Suppressing the influence of CCD vertical blooming on M^2 determination through deep learning. In Proceeding of the 18th International Conference on Optical Communications and Networks (ICOCN) (2019). Huangshan China.

29. An Y, Li J, Huang L, Leng J, Yang L, Zhou P. Deep learning enabled superfast and accurate M^2 evaluation for fiber beams. *Opt Express* (2019) 27:18683–94. doi:10.1364/oe.27.018683

30. Jiang M, An Y, Huang L, Li J, Leng J, Su R, et al. M^2 factor estimation in few-mode fibers based on a shallow neural network. *Opt Express* (2022) 30:27304–13. doi:10.1364/oe.462170

31. Snyder AW, Love JD. *Optical waveguide theory*. Chapman & Hall (1983).

32. Siegman AE. How to (maybe) measure laser beam quality. *OSA TOPS* (1998) 17: 184–99.

33. Sprangle P, Ting A, Peñano J, FischerRIncoherent Combining HB, Propagation A. Incoherent combining and atmospheric propagation of high-power fiber lasers for directed-energy applications. *IEEE J Quan Electron* (2009) 45:138–48. doi:10.1109/jqe.2008.2002501

34. Cai Y. Propagation of various flat-topped beams in a turbulent atmosphere. *J Opt A: Pure Appl Opt* (2006) 8:537–45. doi:10.1088/1464-4258/8/6/008

35. Chu X, Liu Z, Wu Y. Propagation of a general multi-Gaussian beam in turbulent atmosphere in a slant path. *J Opt Soc Am A* (2008) 25:74–9. doi:10.1364/josaa.25.000074

36. Ji X, Li X. M^2-factor of truncated partially coherent beams propagating through atmospheric turbulence. *J Opt Soc Am A* (2011) 28:970–5. doi:10.1364/josaa.28.000970

37. Zhi D, Tao R, Zhou P, Ma Y, Wu W, Wang X, et al. Propagation of ring Airy Gaussian beams with optical vortices through anisotropic non-Kolmogorov turbulence. *Opt Comm* (2017) 387:157–65. doi:10.1016/j.optcom.2016.11.049

38. Zhou Y, Huang K, Zhao D. Changes in the statistical properties of stochastic anisotropic electromagnetic beams propagating through the oceanic turbulence. *Appl Phys B* (2012) 109:289–94. doi:10.1007/s00340-012-5173-8

39. Zervas MN, Codemard CA. High power fiber lasers: A review. *IEEE J Sel Top Quan Electron* (2014) 20.

40. Tao R, Wang X, Zhou P. Comprehensive theoretical study of mode instability in high-power fiber lasers by employing a universal model and its implications. *IEEE J Sel Top Quan Electron* (2018) 24.

41. Wan P, Yang L, Liu J. All fiber-based Yb-doped high energy, high power femtosecond fiber lasers. *Opt Express* (2013) 21:29854–9. doi:10.1364/oe.21.029854

42. Teh PS, Lewis RJ, Alam S, Richardson DJ. 200 W Diffraction limited, single-polarization, all-fiber picosecond MOPA. *Opt Express* (2013) 21:25883–9. doi:10.1364/oe.21.025883

43. Fang Q, Li J, Shi W, Qin Y, Xu Y, Meng X, et al. 5 kW near-diffraction-limited and 8 kW high-brightness monolithic continuous wave fiber lasers directly pumped by laser diodes. *IEEE Photon J* (2017) 9:1–7. doi:10.1109/jphot.2017.2744803

44. Zheng J, Zhao W, Zhao B, Hou C, Li Z, Li G, et al. 4.62 kW excellent beam quality laser output with a low-loss Yb/Ce co-doped fiber fabricated by chelate gas phase deposition technique. *Opt Mater Express* (2017) 7:1259–66. doi:10.1364/ome.7.001259

45. Tao R, Xiao H, Zhang H, Leng J, Wang X, Zhou P, et al. Dynamic characteristics of stimulated Raman scattering in high power fiber amplifiers in the presence of mode instabilities. *Opt Express* (2018) 26:25098–110. doi:10.1364/oe.26.025098

46. Ma P, Xiao H, Meng D, Liu W, Tao R, Leng J, et al. High power all-fiberized and narrow-bandwidth MOPA system by tandem pumping strategy for thermally induced mode instability suppression. *High Power Laser Sci Engineerin* (2018) 6:e57. doi:10.1017/hpl.2018.51

47. Xiao H, Li R, Chen Z, Xi X, Wu H, Leng J, et al. 10 kW counter-tandem-pumped fiber laser with high beam quality. *Acta Optica Sinica* (2022) 42:3788.

48. Marcuse D. Curvature loss formula for optical fibers. *J Opt Soc Am* (1976) 66: 216–20. doi:10.1364/josa.66.000216

49. Schermer R, Cole J. Improved bend loss formula verified for optical fiber by simulation and experiment. *IEEE J Quan Electron* (2007) 43:899–909. doi:10.1109/jqe.2007.903364

50. Cheng W, Haus JW, Zhan Q. Propagation of vector vortex beams through a turbulent atmosphere. *Opt Express* (2009) 17:17829–36. doi:10.1364/oe.17.017829

51. Eyyuboğlu HT, Voelz D, Xiao X. Scintillation analysis of truncated Bessel beams via numerical turbulence propagation simulation. *Appl Opt* (2013) 52:8032–9. doi:10.1364/ao.52.008032

52. Tao R, Huang L, Zhou P, Si L, Liu Z. Propagation of high-power fiber laser with high-order-mode content. *Photon Res* (2015) 3:192–9. doi:10.1364/prj.3.000192